Anomalous magnetoresistance near the metamagnetic transition in Gd_2In

1997 J. Phys.: Condens. Matter 9 3763

(http://iopscience.iop.org/0953-8984/9/18/015)

J. Phys.: Condens. Matter **9** (1997) 3763–3777. Printed in the UK PII: S0953-8984(97)79785-6

Anomalous magnetoresistance near the metamagnetic transition in Gd_2In

P A Stampe†, X Z Zhou†, H P Kunkel†, J A Cowen‡ and Gwyn Williams†‡

† Department of Physics, University of Manitoba, Winnipeg R3T 2N2, Canada

‡ Centre for Fundamental Materials Research, Department of Physics and Astronomy, Michigan State University, East Lansing, MI 48824-1116, USA

Received 21 November 1996

Abstract. Gd_2In, a layered intermetallic compound, displays two magnetic phase transitions below room temperature, the lower one being a metamagnetic transition occurring near 100 K. We have completed measurements of both zero-field resistivity for $1.5 \leqslant T \leqslant 300$ K and the magnetoresistance in fields of up to 8 T for temperatures between 1.5 and 120 K; in addition the magnetization has been studied in fields up to 5.5 T in the temperature range $2 \leqslant T \leqslant 140$ K. As the spin configuration in the ordered phases remains uncertain, these measurements concentrate on the behaviour near the 'ferromagnetic-to-antiferromagnetic' transition, and as such they can be compared and contrasted with those reported recently for Ru-doped $CeFe_2$ in which the spin configurations are better known. Plots of the metamagnetic field as a function of temperature yield metamagnetic transition temperatures of between 94 and 96 K (in zero field), in good agreement with earlier estimates. Additional features are observed below 100 K in this system, suggesting differences between Gd_2In and the doped $CeFe_2$ system, originating possibly from fundamental differences in spin structure.

1. Introduction

Gd_2In has a filled NiAs structure ($P6_3/mmc$), the hexagonal unit cell of which contains two formula units, arranged in a layered ABACA structure stacked along the c-axis. The A layers, at positions 0 and $c/2$, contain only Gd atoms, located at the cell corners, while crystallographically inequivalent B and C layers, at positions $c/4$ and $3c/4$ respectively, each contain one Gd and one In atom within the unit cell [1]. This structure is different from that of $Ce(Fe_{1-x}M_x)_2$, M = Co, Al, Ru, which has a cubic Laves phase structure, with the magnetic Fe atoms located in sheets along (111)-type planes [2]. The ordered magnetic states in $Ce(Fe_{1-x}Ru_x)_2$ are fairly simple, with the Fe spins in each individual (111) plane aligning ferromagnetically. As the temperature is lowered through the metamagnetic transition, while the *intra*-sheet interactions remain ferromagnetic, the *inter*-sheet coupling switches from ferromagnetic to antiferromagnetic, and the lattice undergoes rhombohedral distortion. The more complicated crystallographic structure of Gd_2In precludes such simple arrangements of Gd moments. Furthermore, whereas a Hund's rule ground state of the Gd^{3+} ion ($^8S_{7/2}$) implies a spin-only moment at the Gd site, the corresponding assignment for Ce is currently unclear. The ground state associated with a Ce^{3+} ($4f^1$) configuration is $^2F_{5/2}$ (in a scheme in which spin–orbit coupling is strong); however, band-structure [3] and neutron scattering [2] results indicate that the orbital moment at the Ce site is much lower than that suggested by the Hund's rule ground state, due possibly to hybridization and crystalline-field effects [3].

0953-8984/97/183763+15$19.50

The behaviour of both the magnetization and resistivity in Gd_2In [4–6] does, however, exhibit considerable similarities to those reported for $Ce(Fe_{1-x}Ru_x)_2$ [7, 8]. At high temperature both systems are paramagnetic, with ferromagnetism developing as the temperature is lowered through T_c (190 K in Gd_2In). As the temperature is lowered further, a second anomaly is observed; in both systems the resistivity displays a sharp increase—similar to that associated with superzone effects—and the magnetization exhibits a sudden fall. The zero-field ac susceptibility, $\chi_{ac}(0, T)$, remains large in Gd_2In immediately below this second transition [9] while in doped $CeFe_2$ it does not [10]. Such features are consistent with a second phase transition to a state whose structure is currently unknown in Gd_2In. An applied magnetic field suppresses this transition to lower temperatures, and moderately high fields can completely restore the ferromagnetic state in Gd_2In [4–6]. $Ce(Fe_{1-x}Ru_x)_2$ also shows metamagnetic behaviour, with the applied field pulling the moments on adjacent sheets from the antiparallel configuration to the parallel, ferromagnetic configuration [7, 8]; however, available fields cannot drive this transition below about 60 K. While a similar spin reorientation has been suggested for Gd_2In, the precise structures of the ferromagnetic and antiferromagnetic states are unknown. Mössbauer spectroscopy of ^{119}Sn substituted at the In sites was interpreted as showing ferromagnetic Gd–Gd coupling in *both* of the lower states [11]. This is in apparent contradiction of magnetic measurements, in which a sharp drop in magnetization below 100 K presumably indicates *some* antiferromagnetic alignment. Jee *et al* [6] suggest, on the basis of the low-field behaviour of their magnetization curves, that the system is not a simple ferromagnet from 100–190 K, and propose a spiral ferromagnetic structure similar to that found in MnSi [12]. McAlister, however, suggested a simple ferromagnetic structure, with the moments lying in the basal plane, as is the case in Tb_2In (which has a similar crystallographic structure). Further, McAlister argued that since the Gd moments in the A, B and C planes are in different environments, the simple antiferromagnetic layer–layer coupling, seen for example in $Ce(Fe_{1-x}Ru_x)_2$, would result in ferrimagnetic rather than antiferromagnetic ordering. Low-temperature magnetization measurements of Sm_2In [13], which is known to order ferrimagnetically, show different behaviour from similar measurements on Gd_2In, suggesting that Gd_2In is not ferrimagnetic, but could have a spiral antiferromagnetic structure [4]. In the latter the Gd moments may or may not lie in the basal plane. Due to the high absorption cross-section of gadolinium for thermal neutrons, no neutron diffraction measurements have been attempted from which the true magnetic structure of the low-temperature phases might be determined. With this in mind, we have undertaken a detailed study of the magnetization and magnetoresistance in the vicinity of the lower transition in Gd_2In, an extended analysis of the field dependence of the ac susceptibility near the upper, ferromagnetic transition having been reported previously [9]. These data are compared and contrasted to those previously taken on $Ce(Fe_{1-x}Ru_x)_2$, $x = 0.07$, 0.08, samples whose magnetic structure is known, the assumption being that such a comparison might be useful in elucidating the spin ordering in Gd_2In.

Indeed, a quantitative understanding of the relationship between the magnetic and transport properties of these relatively simple naturally layered intermetallic compounds would seem to be a prerequisite to attempting to model the more complex situation encountered recently [14] in perovskite structures displaying colossal magnetoresistance associated with both charge and spin ordering.

2. Experimental details

The specimen used in both the magnetization and magnetoresistance measurements was a piece cut from a sample used earlier in an ac susceptibility study [9]. This sample

was prepared by McAlister, and details of sample preparation techniques have been given previously [4]. The sample was a brittle, rectangular bar weighing 65.2 mg, with dimensions $11.9 \times 0.9 \times 0.7$ mm^3.

Resistivity measurements were performed using a high-sensitivity ac technique [15], which achieves a relative accuracy of better than one part in 10^4, with an ac measuring current (50 mA, 37 Hz) applied along the longest sample dimension. The uncertainty in the absolute value of the resistivity can be as large as 10%, due primarily to difficulties in obtaining precise form factors as well as systematic errors inherent in the ac technique. The temperature dependence of the resistivity from 1.5 K to 300 K was measured in zero field, and between 4.2 K and 115 K in a fixed magnetic field of 7.2 T applied parallel to the measuring current. The field dependence of the resistivity was measured at 15 fixed temperatures in the range $1.5 < T < 115$ K, in fields of up to 8.4 T.

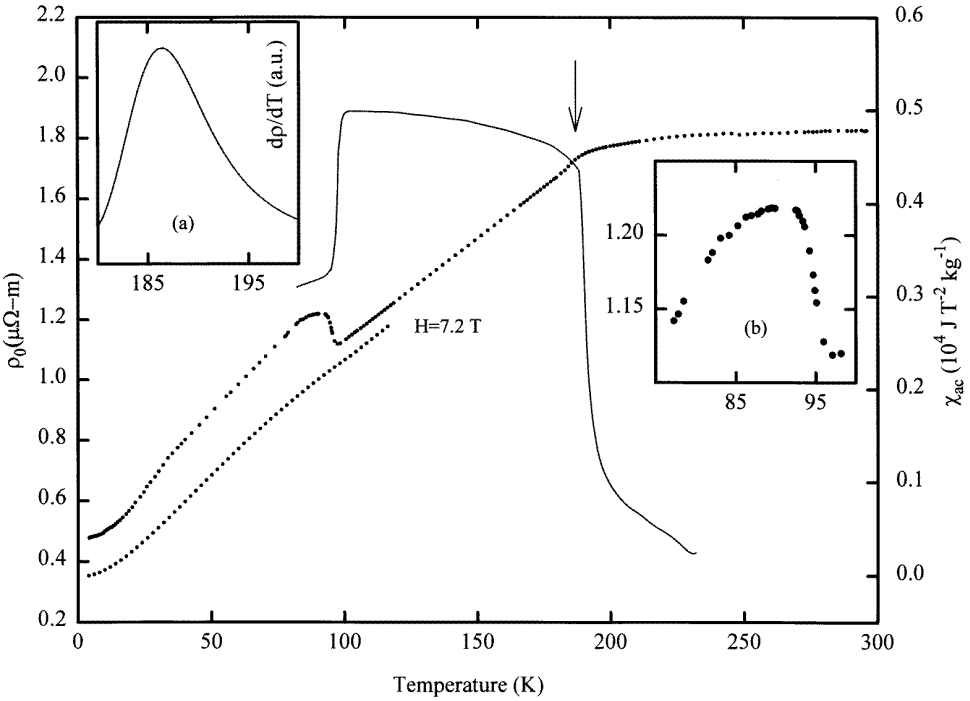

Figure 1. The resistivity $\rho(H, T)$ (in $\mu\Omega$ m) plotted against temperature (in K) for fixed applied fields of zero (upper data set) and 7.2 T (lower data set); the solid line represents the zero-field ac susceptibility [9, 16] with the vertical arrow indicating T_c estimated from these susceptibility data. Inset (a) shows the derivative of the zero-field resistivity data in the vicinity of T_c while inset (b) reproduces the zero-field resistivity data near the lower transition on an expanded scale.

Magnetization measurements were taken with a commercial SQUID magnetometer (Quantum Design MPMS5) with the biasing field along the longest sample dimension. Data acquisition was performed using a 64-step, 4 cm scan. Reducing the step number caused the measured saturation moment to fall, an effect attributed to the unlocking of the SQUID system due to a high slew rate caused by the large saturation magnetization of 1300 emu cm^{-3} of this system (a value approaching that of Co). The use of the same sample in both magnetoresistance and magnetization measurements allows direct comparison

between data points at a fixed applied field and temperature in both sets of data. $M(H)$ curves were measured at a number of fixed temperatures from 1.5 to 140 K. The sample was warmed above T_c (200 K) and cooled in zero field prior to each field sweep to ensure consistent initial conditions.

3. Results and discussion

3.1. General features

Figure 1 reproduces the general features of the transport measurements along with the previously measured ac susceptibility [9]. The zero-field resistivity $\rho(0, T)$ is in good overall agreement with that reported by McAlister [4], and the features evident in the latter correspond well with characteristic features in the zero-field ac susceptibility $\chi_{ac}(0, T)$. The vertical arrow in this figure marks the ferromagnetic ordering temperature T_c ($=187 \pm 1$ K) deduced from an analysis of the susceptibility data $\chi_{ac}(H, T)$ [9], and this correlates well with the abrupt change in slope of $\rho(0, T)$ which characterizes this transition in the zero-field resistivity. This connection is made in a more quantitative manner via the inset (a) in this figure, which shows the derivative $\mathrm{d}\rho/\mathrm{d}T$ of the zero-field curve. The maximum in this derivative yields $T_c = 186.5 \pm 1$ K, in good agreement with that listed above and with the value of 187 ± 3 K reported by McAlister using the derivative method. All estimates were made on pieces cut from the same initial sample.

In the vicinity of the lower, metamagnetic transition, $\rho(0, T)$ exhibits a rapid increase with decreasing temperature (shown in more detail in the second inset (b) in figure 1), the onset of which, at 96 ± 1 K, correlates very well with the mid-point (96 ± 1 K) of the sharp fall in $\chi_{ac}(0, T)$ and with the peak in the temperature dependence of the coefficient $a_2(T)$ of the leading field-dependent contribution to the susceptibility ($\chi(H, T) = \chi(0, T) + a_2(T)H^2 + \cdots$) [16]. McAlister has estimated the metamagnetic transition temperature T_m as 99.5 ± 1 K from the low-temperature anomaly in $\mathrm{d}\rho/\mathrm{d}T$ (essentially equivalent to taking T_m at the onset of the sudden increase in $\rho(T)$). The behaviour of $\rho(0, T)$ in this region is reminiscent of that often associated with superzone effects in a variety of systems (including Ru-doped $CeFe_2$ [7, 8]), and the detailed measurements reported below were carried out in the vicinity of this second transition.

The lower-resistivity curve shown in figure 1 indicates the effects of an external field of 7.2 T for temperatures between 1.5 and 120 K (the highest temperature attainable in the present cryostat when the magnet is in persistent mode near full field). The effects of this field are striking, and demonstrate in a direct manner the behaviour inferred from previous magnetization studies [4–6], namely that a (moderately) high field can completely suppress this metamagnetic transition (at least above 1.5 K). In the ferromagnetic regime this field produces a much weaker magnetoresistance—as expected—discussed in more detail below.

3.2. Magnetoresistance

A detailed examination of the lower transition has been carried out by measuring the field dependence of the resistivity $\rho(H, T)$ at 15 fixed temperatures below 120 K in fields up to 8.5 T. The low-field portions of seven such curves are reproduced in figure 2, in which the fractional magnetoresistance $\Delta\rho/\rho_0 = (\rho(H, T) - \rho(0, T))/\rho(0, T)$ is plotted against the applied field. These curves resemble those measured previously for Ru-doped $CeFe_2$ [7, 8], in that a *single* transition between two magnetic states is observed, with no intermediate states as have been reported recently for perovskite structures [14].

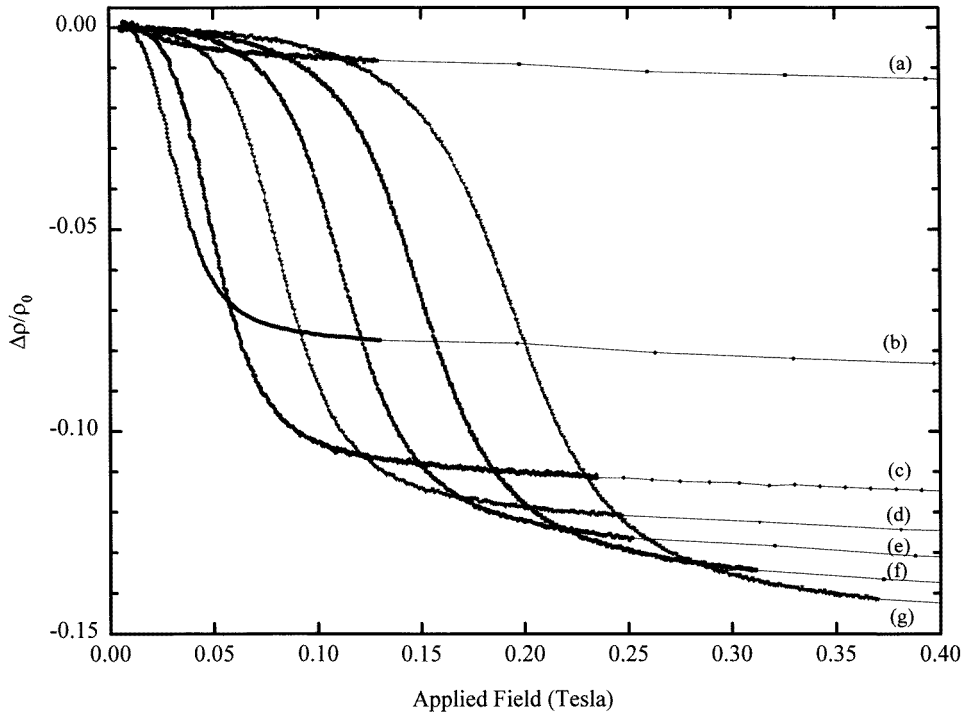

Figure 2. The magnetoresistance ratio $\Delta\rho/\rho_0$ $(=[\rho(H,T)-\rho(0,T)]/\rho(0,T))$ plotted against the applied field (in T) at fixed temperatures of (a) 98.8 K, (b) 96.0 K, (c) 92.7 K, (d) 90.2 K, (e) 87.9 K, (f) 84.6 K and (g) 81.3 K.

In the ferromagnetic phase at temperatures above the lower transition, at 98.8 K for example, the magnetoresistance is small and negative. A small ($\sim -6\%$ at 7.2 T) magnetoresistance at this temperature is consistent with the conjectured ferromagnetic structure, the internal field from which is expected to have reduced substantially spin-disorder scattering effects, with the result that the subsequent influence of large external fields is minimal. At temperatures below the metamagnetic transition the results are quite different; in figure 2(g) at 81.3 K, the magnetoresistance is seen to exhibit a plateau region at low field, above which a sharp fall in the resistivity occurs. The latter indicates that the field has reached the critical value $H_m(T)$ necessary to drive the metamagnetic transition at that temperature. At still higher fields the magnetoresistance becomes much weaker, exhibiting a small but continuous drop to the highest field available; this result is again consistent with a field-induced reduction in the number of thermally generated magnons in the restored ferromagnetic state. As can be seen from figure 2, the fractional, field-induced change in the resistivity increases with decreasing temperature below the lower transition, with the high-field value for $\Delta\rho/\rho_0$ increasing from about 8.5% at 96 K to 14% near 81.3 K. Basically, this results—as can be seen from figure 1—from the divergence between $\rho(0,T)$ and $\rho(7.2\ \mathrm{T},T)$ in this temperature region. As the temperature decreases further, this fractional change continues to increase, reaching a value near 29% at 4.2 K (figure 3). This increase arises from a reduction in the zero-field resistivity $\rho(0,T)$ since the field-induced change $\Delta\rho(H,T)=\rho(0,T)-\rho(H,T)$ in high field is relatively insensitive to temperature below 70 K (figure 1). Although not reproduced in figure 3, the magnetoresistance at

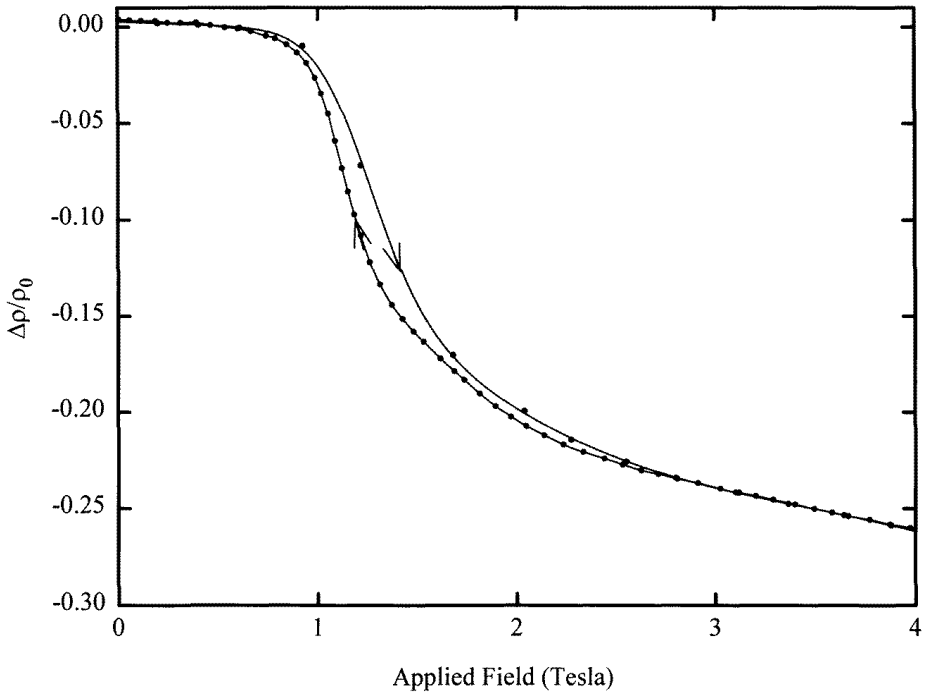

Figure 3. The fractional magnetoresistance $\Delta\rho/\rho_0$ plotted against the applied field (in T), showing the hysteresis effects, at a fixed temperature of 4.2 K.

4.2 K is saturated in fields above 5–6 T, which would suggest that complete ferromagnetic alignment has been restored—at least on length scales on the order of the mean free path (which is admittedly short in this system). While the overall features of the curves shown in figures 2 and 3 are similar to those reported previously for Ru-doped $CeFe_2$ [7, 8], there are differences in detail, as discussed below.

3.3. Hysteresis

Figure 3 reproduces the magnetoresistance of Gd_2In at 4.2 K measured in both increasing and decreasing field. The observed hysteresis at this temperature is clearly quite small, as the width of the loop depicted is less than 0.1 T. This is in marked contrast to other 'layered' structures that have been measured, with $CeFe_2$ doped with either Ru or Al [7, 8, 17] displaying a marked hysteresis in $\rho(H, T)$ in the antiferromagnetic phase. For example, in $Ce(Fe_{0.93}Ru_{0.07})_2$ this width has already risen to approximately 0.2 T close to the *onset* of the zero-field resistive transition at $\sim$115 K; at 60 K the loop width exceeds 0.6 T. In general, hysteretic loop widths measure the coercive field, and these large differences between the coercive field in Gd_2In and doped $CeFe_2$ are most likely attributable to the absence of an orbital moment at the Gd site, as single-ion spin–orbit coupling in conjunction with crystal fields is an often-cited source of magnetic anisotropy. It is also possible that structural differences between these two systems could influence the mechanism driving the metamagnetic transition (accompanied by a structural distortion in doped $CeFe_2$ [2]), hence affecting any associated hysteresis.

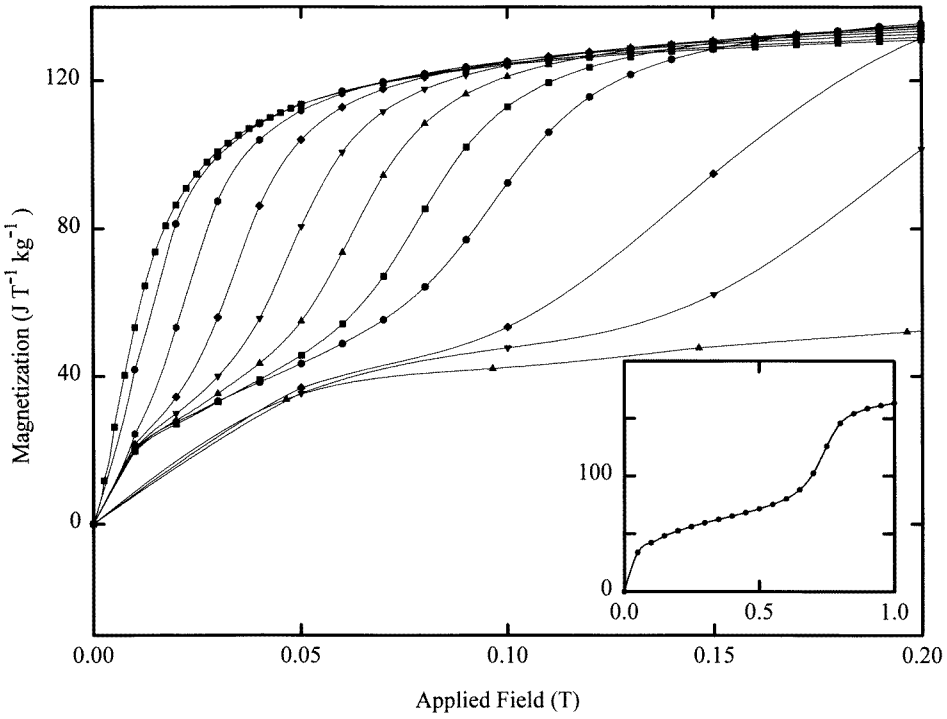

Figure 4. The lower-field magnetization (in J T^{-1} kg^{-1}) acquired near and below T_m, plotted against the applied field (in T) at fixed temperatures of (from left to right) 99 K, 97 K, 95 K, 93 K, 91 K, 89 K, 87 K, 85 K, 80 K, 75 K and 15 K. The inset shows similar data at 4.2 K.

3.4. Magnetization

The main body of figure 4 reproduces eleven magnetization curves acquired in the vicinity of T_m and below on the same sample used in the transport measurements, with fields applied along the same (longest) dimension. The inset shows magnetization data at 4.2 K (i.e. well below T_m). From this inset it can be seen that as the field is increased the magnetization initially increases rapidly, before entering a plateau regime. With further increases in field this plateau terminates abruptly as the magnetization again rises rapidly. As in doped $CeFe_2$ [7, 8, 17], this increase in magnetization beyond the plateau is taken as indicating the onset of the field-driven metamagnetic transition, and this feature can be used to estimate the temperature-dependent metamagnetic field $H_m(T)$, as has been done previously [7, 8, 17] and described in more detail below. Beyond this metamagnetic field the slope of the magnetization curve falls substantially, but this slope does not fall to zero in available fields, indicating incomplete saturation in a 5.5 T field, even at 4.2 K. Before discussing this latter feature in detail, it is interesting to compare and contrast the data displayed in figure 4 with those reported for $Ce(Fe_{0.93}Ru_{0.07})_2$; though they are basically quite similar there are differences in the nature of the detailed response. Both systems exhibit a rapid increase in the initial magnetization with field, the origin of which is currently unknown. It was suggested [7] that it *might* result from a small non-collinearity in the ferromagnetic Fe (111)-sheet alignment induced by Ru or Al substitutional replacement in doped $CeFe_2$, this local non-collinearity being orientable in fields generally smaller than $H_m(T)$. This

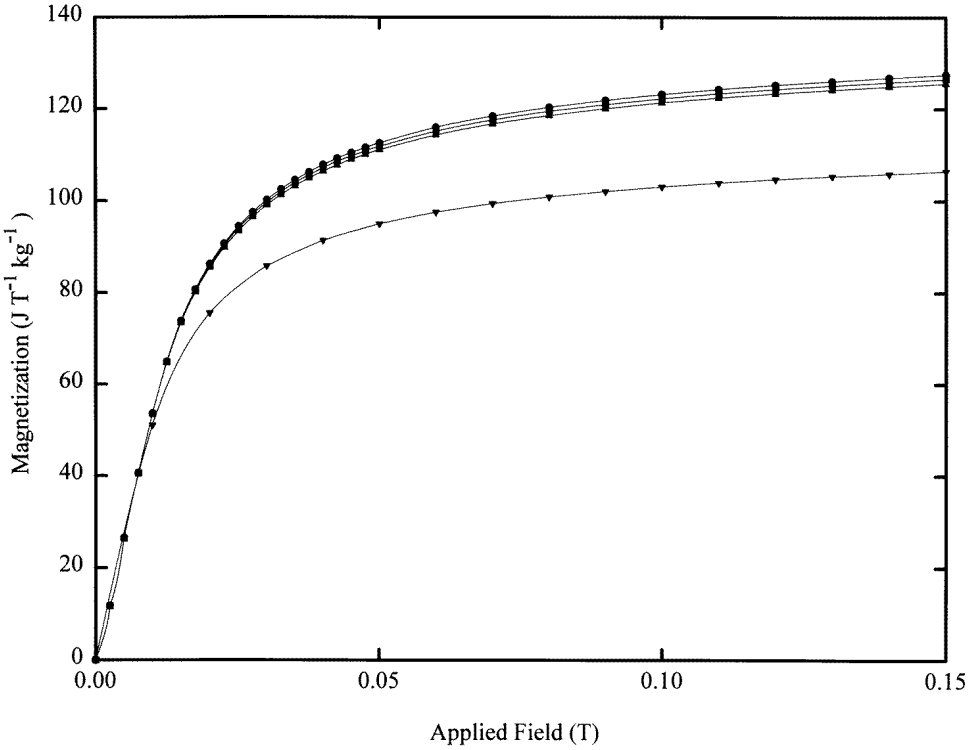

Figure 5. The lower-field magnetization (in J T^{-1} kg^{-1}) measured in the ferromagnetic phase plotted against the applied field (in T) at fixed temperatures of (from top to bottom) 101 K, 103 K, 105 K and 140 K.

possibility is clearly not appropriate for undoped Gd_2In, although slight departures from stoichiometry might be responsible. This initial increase gives way to the plateau regime, the onset of which occurs at *much* lower fields in Gd_2In. The latter, coupled with a substantially larger initial magnetization, results in a considerably enhanced susceptibility in this system, reflected directly in the magnitude of the ac susceptibility immediately below the lower transition. $\chi_{ac} \sim 3 \times 10^3$ J T^{-2} kg^{-1} near 90 K in figure 1, compared with $\sim$10 J T^{-2} kg^{-1} near 70 K in $Ce(Fe_{0.93}Ru_{0.07})_2$ [7], suggesting far less magnetic rigidity in the low-temperature spin structure established here. This feature persists into the plateau regime, which is essentially flat in doped $CeFe_2$ throughout the antiferromagnetic regime [7, 8]. This is in contrast with the behaviour evident in figure 4; in Gd_2In the 'plateau' has a noticeable slope even at 4.2 K (the inset in figure 4). This slope increases monotonically with increasing temperature as the magnetization curve evolves into a 'normal' form above the lower transition (the highest-temperature curve among those shown in figure 4).

A number of magnetization curves measured in the ferromagnetic regime are plotted in figure 5. As observed by Jee *et al* [6] these curves appear to exhibit a limiting low-field slope, with data acquired at different temperatures falling on the same line. A similar result was reported by McAlister [4]; however, there this limiting slope corresponded to the demagnetization-factor-limited behaviour expected from a spherical sample. In the present work the demagnetization factor N was estimated by approximating the specimen by an ellipsoid with principal axes equal to the measured dimensions; from the corresponding

elliptic integrals [18] one obtains $N \sim 1.2\times10^{-4}$ T^2 kg J^{-1}. This estimate yields a calculated limit for the low-field slope of $N^{-1} \sim 8600$ J T^{-2} kg^{-1}, a limit that is higher than the measured value of 6000 J T^{-2} kg^{-1} from figure 5. Nevertheless, due to the non-ideal sample shape (with its attendant effects on both the uncertainty in the calculated demagnetization factor and the non-uniformity of the internal field) we cannot state definitively that this slope is *not* limited by the demagnetization factor. Thus these data do not support the suggestion of Jee *et al* [6] that such behaviour results from the magnetic spin configuration in this temperature regime (particularly as the limiting slope evident in figure 5 is some 15 times *larger* than that reported by Jee *et al*).

By contrast, the high-field slopes of these magnetization curves do provide information on the spin structure and its approach to complete collinearity, as mentioned earlier. However, before discussing this aspect of the present magnetization data in detail, it is worthwhile to compare the behaviour of Gd_2In and doped $CeFe_2$ with that reported for manganese perovskites, specifically the half-doped $La_{0.5}Ca_{0.5}MnO_{3+\delta}$ system [14]. The virgin curves in the latter exhibit the ubiquitous low-field increase evident in figure 4, the magnitude of which ($\sim$10 J T^{-2} kg^{-1}) is comparable with that in doped $CeFe_2$. The plateau region beyond this low-field increase, by contrast, displays more similarity to the case for Gd_2In. The slope of this region increases, while its range in field decreases, as the temperature increases, although the slope of this plateau is nearly two orders of magnitude larger for Gd_2In—a result related primarily to the much wider field range associated with this behaviour in $La_{0.5}Ca_{0.5}MnO_{3+\delta}$ (some 10 T at 4.2 K; c.f. the $<$1 T field evident in the inset in figure 4). The pronounced difference between this perovskite and the metallic systems considered here lies in the width of its 'hysteresis' loops—of the order of 10 T at 4.2 K. Such widths do not arise from traditional magnetic sources, but from the metastability of the ferromagnetic state which, once established, remains locked in through a combination of spin- and charge-ordering effects [14].

To return to the present magnetization data, the $M(H)$ plots for Gd_2In display continuous curvature in fields up to 5.5 T (the largest available in the MPMS5 system) at all temperatures, so the magnetization is not linear in either H or H^{-1} in the high-field region. The estimates discussed below are thus obtained subject to this constraint. The high-field slope of these $M(H)$ plots is large, the average slope (estimated between 4.5–5.5 T; see the inset in figure 6) decreasing essentially monotonically from around 2 J T^{-2} kg^{-1} at 140 K to some 0.5–0.6 J T^{-2} kg^{-1} in the liquid helium range. This latter value is an order of magnitude larger than that for Pd, a well-known example of a Pauli paramagnet with substantial exchange enhancement. These slopes are thus unlikely to originate from band-structural sources; their most likely origin lies in some non-collinearity in the Gd spin configuration. Estimates have also been made of the saturation moment at various temperatures using an extrapolation based on the highest-field points in an M versus H^{-1} plot. These moments increase with decreasing temperature from around $5.5\mu_B$/Gd at 140 K to approximately $7.2\mu_B$/Gd at and below 4.2 K. While the latter is some $0.2\mu_B$/Gd higher than that expected from the bare Gd moment, it should be recalled that the magnetoresistance at 4.2 K does saturate rapidly in fields above 5–6 T. Should a similar situation occur for the magnetization, then the saturation moment at this temperature would fall to $7.1\mu_B$/Gd. With these points in mind, in figure 6 we summarize the fractional magnetoresistance $\Delta\rho(H,T)/\rho_0$ at 1.5 and 4.2 K to 8.4 T; the inset presents the highest-field magnetization data $M(H,T)$ acquired at 2 K, the lowest attainable temperature in this cryostat. Close examination of $\rho(H,T)$ indicates a marked and abrupt flattening beyond 5–6 T at both temperatures, but the $M(H,T)$ measurements at 2 K do not, despite a careful re-examination of data for the 4.5–5.5 T range, as shown in the inset. This result is what might be anticipated

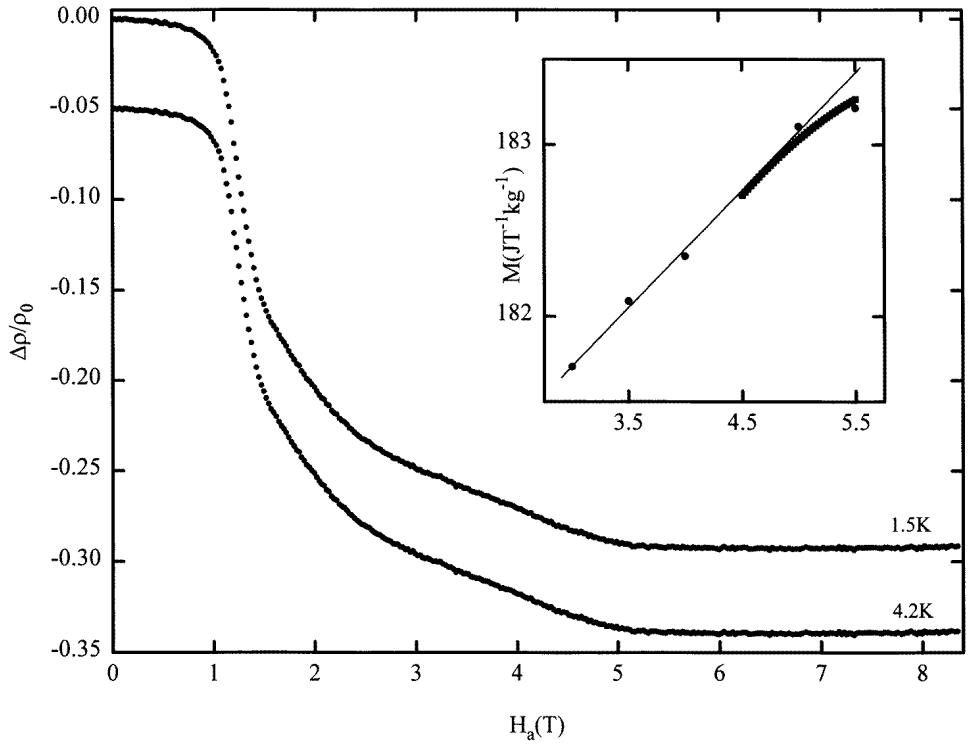

Figure 6. The fractional magnetoresistance $\Delta\rho/\rho_0$ plotted against the applied field H_a (in T) over the full available field range, at fixed temperatures of 4.2 K and 1.5 K. These data saturate between 5 and 6 T. The inset reproduces the high-field magnetization (in J T^{-1} kg^{-1}) at 2 K with the results of a careful remeasurement between 4.5 and 5.5 T.

considering the nature of the two measurements; that is, the magnetization—being a global measurement—should reveal saturation effects after the magnetoresistance, as the latter property probes the spin structure on a length scale of the order of the (inelastic) mean free path. Measurements of the magnetization in fields higher than those currently available to us are clearly necessary to investigate this situation more carefully, although macroscopic measurements of the type described here will not yield direct information on the microscopic spin configuration.

3.5. The temperature dependence of $H_m(T)$

Estimates for the metamagnetic field, $H_m(T)$, as a function of temperature have been extracted from the $\rho(H,T)$ and $M(H,T)$ data using two approaches. The first approach, introduced by Radha *et al* [17] in an analysis of the behaviour of Al-doped $CeFe_2$, identifies H_m as that field at which the magnetoresistance first becomes negative or at which the magnetization first begins to increase rapidly (beyond the plateau region). The second approach, a more quantitative estimate in our opinion [7], associates H_m with the field at which $\rho(H,T)$ or $M(H,T)$ exhibits the largest slope (at a given temperature). This latter approach is summarized in figure 7 (these slopes were calculated by fitting the corresponding curves to an (arbitrary) analytic function and then differentiating with respect to field, as

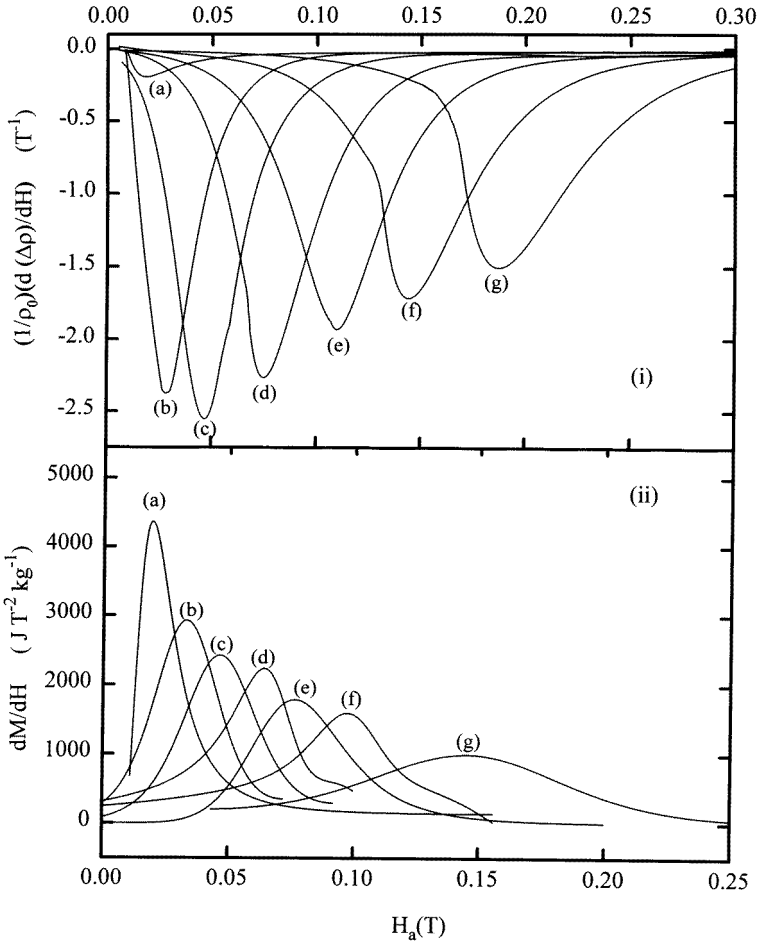

Figure 7. The derivatives $(1/\rho_0)(\mathrm{d}\,\Delta\rho/\mathrm{d}H)$ (in T^{-1}) and $\mathrm{d}M/\mathrm{d}H$ (in $\mathrm{J\,T^{-1}\,kg^{-1}}$) plotted against the applied field H_a (in T) at fixed temperatures of (i), upper figure, (a) 98.8 K, (b) 96.0 K, (c) 92.7 K, (d) 90.2 K, (e) 87.9 K, (f) 84.6 K and (g) 81.3 K, and (ii), lower figure, (a) 95 K, (b) 93 K, (c) 91 K, (d) 89 K, (e) 87 K, (f) 85 K and (g) 80 K.

described previously [7]). The location of this maximum slope in both $\rho(H)$ (figure 7(i)) and $M(H)$ (figure 7(ii)) moves to lower field as the temperature approaches T_m from below, as expected. Further, the locations of the maxima in $\mathrm{d}M/\mathrm{d}H$ are consistently lower in field than those from $\mathrm{d}(\Delta\rho/\rho_0)/\mathrm{d}H$ at a given temperature, a result first noted for the Ru-doped $CeFe_2$ system [7, 8]. While such similarities exist, there are again marked differences in the detailed behaviour of these two systems. For doped $CeFe_2$ the magnitudes of these maxima remained essentially constant below 0.9 T_m. As can be seen from figure 7 the behaviour of Gd_2In is quite different; the magnitudes in question essentially increase steadily with increasing temperature over a corresponding interval. In the case of the magnetization data this increase is maintained *through* T_m where it approaches the ferromagnetic limiting slope of 6000 $\mathrm{J\,T^{-2}\,kg^{-1}}$, evident in figure 5 (for purposes of clarity slopes found from $M(H)$ data above 97 K are not included in figure 7(ii)). Such behaviour reflects the evolution in the 'plateau' regime in Gd_2In, discussed above. The peak in $\mathrm{d}M/\mathrm{d}H$ for doped $CeFe_2$

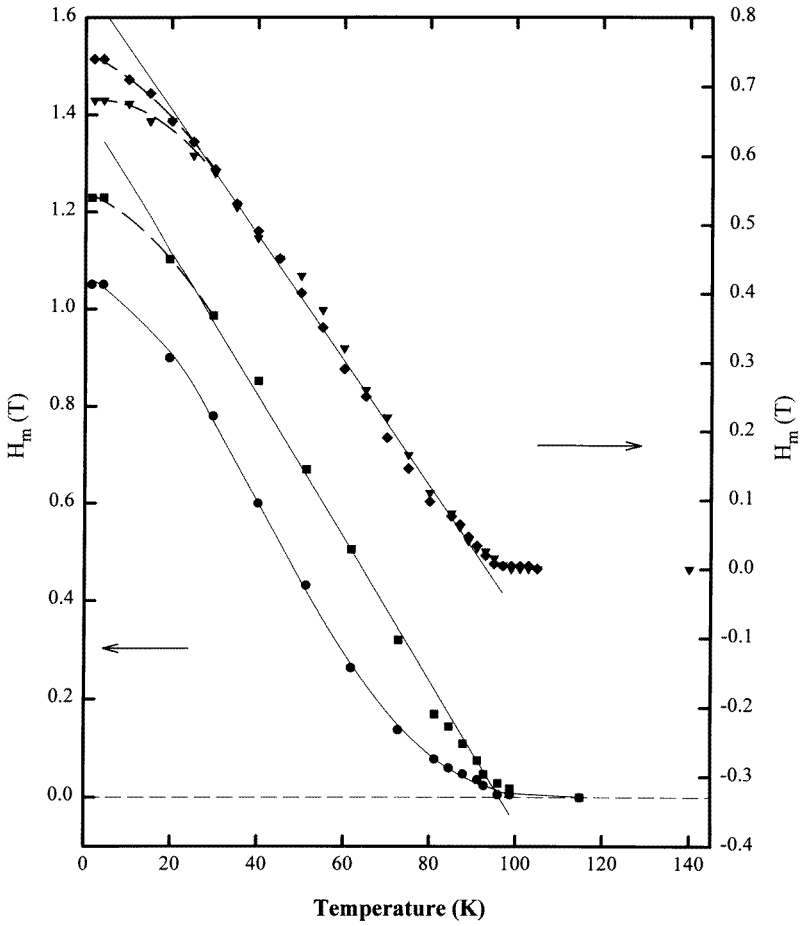

Figure 8. Estimates for the metamagnetic field $H_m(T)$ (in T) plotted against temperature (in K); these estimates were obtained from (i) the onset of a rapid increase in $M(H)$ (▼), (ii) the maximum in $\mathrm{d}M/\mathrm{d}H$ (♦), (iii) the onset of a negative $\rho(H)$ (●), and (iv) the maximum in $(\mathrm{d}\,\Delta\rho/\mathrm{d}H)$ (■). The lines are drawn as guides to the eye.

shows a sudden decline close to T_m, as do the peaks in $\mathrm{d}(\Delta\rho/\rho_0)/\mathrm{d}H$ in both systems. We suggest again that these marked differences could reflect an inequivalence in the associated spin structures.

Figure 8 summarizes the temperature dependence of $H_m(T)$ determined from the two sets of data using the two criteria discussed above. As might be expected, estimates determined using the first criterion lie below those deduced from the second (derivative) method, but only marginally so for the $M(H, T)$ data. The latter indicate an approximately linear variation for $H_m(T)$ with temperature just below T_m, and a fit of these data to the form

$$H_m(T) = a(T_m - T) \tag{1}$$

yields $T_m = 94 \pm 1$ K and $a \simeq 9 \times 10^{-3}$ T K^{-1}. The coefficient a is an order of magnitude smaller than the lowest value reported for doped $CeFe_2$ [7, 8]. This reflects the fact that not only is the zero-temperature value for H_m ($\sim$1 T in Gd_2In) well below that for the doped

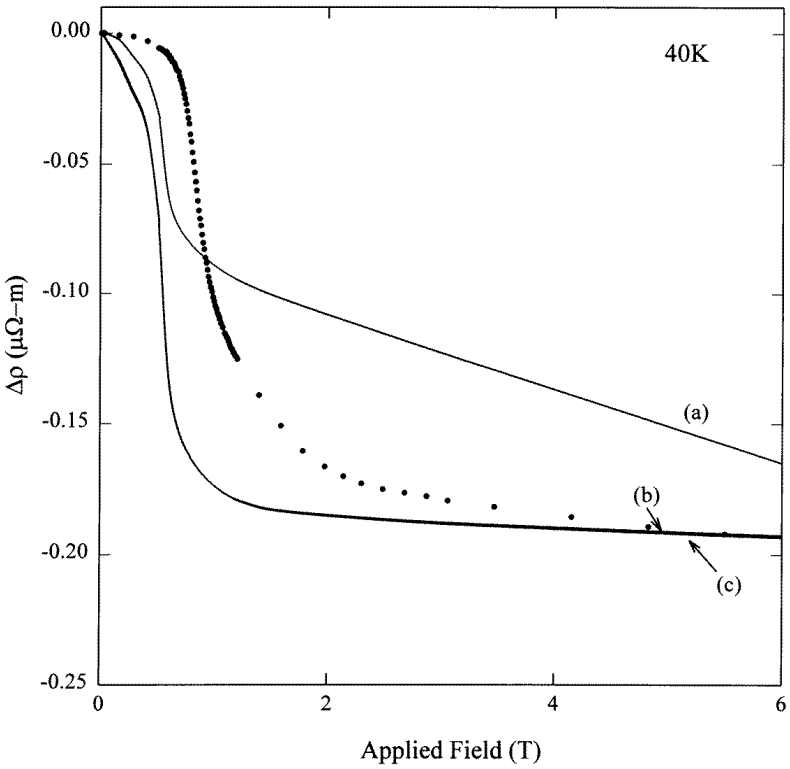

Figure 9. The magnetoresistance $\Delta\rho = \rho(H, T) - \rho(0, T)$ (in $\mu\Omega$ m) plotted against the applied field (in T) at 40 K. Experimental data are represented by (•) while the curves labelled (a), (b) and (c) are based on the s–f model expression utilizing the corresponding approximations for the internal field H_i discussed in the text. In addition, for curve (a) $|J| = 0.33$ eV and $|V| = 0.12$ eV, for curve (b) $|J| = 0.13$ eV and $|V| = 0.12$ eV, while for curve (c) $|J| = 0.33$ eV and $|V| = 0.11$ eV.

systems, but also the absence of an orbital moment at the Gd site suggests less impedance (due to a lack of spin–orbit coupling) to spin reorientation. The magnetoresistance data show a greater difference between the two methods for estimating H_m; in addition the latter estimates display more curvature. Nevertheless the derivative estimates for $H_m(T)$ from $\rho(H)$ data allow a fit to equation (1) to be attempted, and this yields $T_m = 96 \pm 1$ K with $a \sim 15 \times 10^{-3}$ T K^{-1}. As expected, this T_m-value is close to the onset of the abrupt increase in $\rho(0, T)$, and it also correlates well with the midpoint of the low-temperature decrease in $\chi_{ac}(0, T)$ (figure 1), noted previously.

In comparing the present $H_m(T)$ estimates with those obtained from other available data, it should be pointed out that the fields shown in figure 8 are not demagnetization factor corrected. Here the specimen dimensions are not only identical in both data sets, but they have also been chosen specifically to reduce this correction. Thus the largest reduction to the H_m-values shown occurs at 2 K, and even there it does not exceed 0.03 T. The estimates shown in this figure appear to be in reasonable agreement with those found from published magnetization curves [4, 6] utilizing the same criteria as discussed above, once such corrections are made to the latter data.

3.6. The relationship between $\rho(H, T)$ and $M(H, T)$ in an s–f model

As in doped $CeFe_2$ [7, 8], the differences evident between the $H_m(T)$ estimates derived from $\rho(H, T)$ and $M(H, T)$ data have important implications for model-based approaches which attempt to correlate the behaviour of these two properties. The s–f model is typical of such approaches in that it relates $\Delta\rho(H, T) = \rho(0, T) - \rho(H, T)$ and $\langle S_z \rangle \propto M(H, T)$ through the equation [19]

$$\Delta\rho(H, T) = Ac\left[J^2\langle S_z\rangle \tanh\left(\frac{\alpha}{2}\right) + \frac{4V^2J^2\langle S_z\rangle^2}{V^2 + J^2[S(S+1) - \langle S_z\rangle \tanh(\alpha/2)]}\right] \tag{2}$$

where $A = 3m^*\Omega/(2\hbar e^2 E_F)$ depends on the detailed band structure (Ω is the atomic volume, m^* is the conduction electron effective mass, and E_F is the Fermi energy), c is the atomic fraction of scattering sites, and $\alpha = g\mu_B H_i/k_B T$. As an example, the magnetoresistance at 40 K is fitted to equation (2), using $\langle S_z\rangle$-values scaled to the measured magnetization. The value Ac was set at the same value as for the $Ce(Fe_{1-x}Ru_x)_2$ samples previously measured ($Ac = 200$), to allow direct comparison of the fitting parameters. Three different choices for the internal field H_i are utilized in figure 9. They are: (a) $H_i = H_a$; (b) $H_i = H_a + \lambda M$, with the molecular field constant $\lambda = T_N$; and (c) $H_i = H_a + k_B T_N/\mu_B$. Here an alternative approach was taken in fitting this function in that V and J (the directionally averaged potential and exchange coupling strength) were chosen to reproduce the *overall* change in $\Delta\rho(H, T)$ between low and high field (previously [7] a least-squares fit was presented). Curves (b) and (c) mimic the flat low- and high-field behaviour quite well; however, as seen for $Ce(Fe_{1-x}Ru_x)_2$, the curves drop at a much lower field than the measured magnetoresistance, reflecting the different H_m-estimates referred to above. Although the s–f model has been successful in fitting the GMR in granular systems [20], obtained by the rapid freezing of immiscible materials, none of the fits shown here are convincing. This suggests that this model does not accurately reproduce the behaviour near the metamagnetic transition in these intermetallics, probably because magnetoresistive effects in these systems may be related to band-structure changes induced by superzone effects (at least if the situation here is similar to that reported recently for UNiGa [21]). Nevertheless, it remains difficult to understand how the changes in magnetization and magnetoresistance, presumably driven by the same band-structural changes, can show such dramatically different field dependence.

4. Summary and conclusions

In summary, measurements of the magnetization and magnetoresistance in the vicinity of the metamagnetic transition of Gd_2In, while showing many similarities overall to those for the $Ce(Fe_{1-x}Ru_x)_2$ systems measured previously, differ in detailed behaviour both in and below the transition region. Such differences support the suggestion that the low-temperature structure in Gd_2In is different from the simple antiferromagnetism present in $Ce(Fe_{1-x}M_x)_2$, M = Ru, Al, possibly reflecting the more complicated crystallographic structure of Gd_2In. In both types of system the level of agreement between various $H_m(T)$ estimates and the attendant failure of the s–f model to correlate the magnetization with the magnetoresistive response in these relatively simple systems remains puzzling. Nevertheless it would be interesting to investigate the applicability of this model approach to the more complex relationships between electronic transport and magnetic structure displayed by various perovskites.

Acknowledgments

Support for this work from various programmes of the Natural Sciences and Engineering Research Council (NSERC) of Canada is gratefully acknowledged. The work at MSU was supported by the NSF and the MSU Centre for Fundamental Materials Research. One of us (GW) would like to thank the Condensed Matter Physics Group and Michigan State University for support and hospitality during leave in which some of these data were collected.

References

[1] Palenzona A 1968 *J. Less-Common Met.* **16** 379
[2] Kennedy S J and Coles B R 1990 *J. Phys.: Condens. Matter* **2** 1213
Kennedy S J, Brown B J and Coles B R 1993 *J. Phys.: Condens. Matter* **5** 5169
[3] Eriksson O, Nordström L, Brooks M S S and Johansson B 1988 *Phys. Rev. Lett.* **60** 2523
[4] McAlister S P 1984 *J. Phys. F: Met. Phys.* **14** 2167
[5] Gamari-Seale H, Anagnostopoulos T and Yakinthos J K 1979 *J. Appl. Phys.* **50** 434
[6] Jee C S, Lin C L, Mihalisin T and Wang X Q 1996 *J. Appl. Phys.* **79** 5403
[7] Kunkel H P, Zhou X Z, Stampe P A, Cowen J A and Williams G 1996 *Phys. Rev.* B **53** 15 099
[8] Kunkel H P, Zhou X Z, Stampe P A, Cowen J A and Williams G 1996 *Phys. Rev.* B **54** 16 039
[9] Saran M, Williams G and McAlister S P 1986 *Solid State Commun.* **57** 53
[10] Wang D, Kunkel H P and Williams G 1995 *Phys. Rev.* B **51** 2872
[11] Delyagin N N, Mudzhiri G T, Nesterov V I and Reiman S I 1982 *Sov. Phys.–JETP* **59** 592
[12] Motoya K, Yasuoka H, Nakamura Y and Wernick J H 1978 *J. Phys. Soc. Japan* **44** 1525
[13] McAlister S P 1984 *J. Appl. Phys.* **55** 2343
[14] Xiao G, Gond G Q, Canedy C L, McNiff E J Jr and Gupta A 1997 *J. Appl. Phys.* to be published
[15] Muir W B and Ström-Olsen J O 1976 *J. Phys. E: Sci. Instrum.* **9** 163
[16] Cowen J A and Williams G 1997 at press
[17] Radha S, Roy S B, Nigam A K and Chandra G 1994 *Phys. Rev.* B **50** 6866
[18] Osborn J A 1945 *Phys. Rev.* **67** 351
[19] Bews J, Sheikh A W and Williams G 1986 *J. Phys. F: Met. Phys.* **16** 1537
[20] Wang J Q, Xiong P and Xiao G 1993 *Phys. Rev.* B **47** 8341
[21] Antonov V N, Perlov A Ya, Openeer P M, Yaresko A N and Halilov S V 1996 *Phys. Rev. Lett.* **77** 5253